Temperature-Dependent Kinetics of the Vinyl Radical (C_2H_3) Self-Reaction

Huzeifa Ismail[†]

Department of Chemistry, Massachusetts Institute of Technology, Cambridge, Massachusetts 02139

Paul R. Abel[‡,§] **and William H. Green***

Department of Chemical Engineering, Massachusetts Institute of Technology, Cambridge, Massachusetts 02139

Askar Fahr

Department of Chemistry, Howard University, Washington, D.C. 20059

Leonard E. Jusinski, Adam M. Knepp,[‡,||] **Judit Zádor, Giovanni Meloni,**[⊥] **Talitha M. Selby, David L. Osborn, and Craig A. Taatjes***

Combustion Research Facility, Mail Stop 9055, Sandia National Laboratories, Livermore, California 94551-0969

Received: October 30, 2008; Revised Manuscript Received: December 9, 2008

The rate coefficient for the self-reaction of vinyl radicals has been measured by two independent methods. The rate constant as a function of temperature at 20 Torr has been determined by a laser-photolysis/laser absorption technique. Vinyl iodide is photolyzed at 266 nm, and both the vinyl radical and the iodine atom photolysis products are monitored by laser absorption. The vinyl radical concentration is derived from the initial iodine atom concentration, which is determined by using the known absorption cross section of the iodine atomic transition to relate the observed absorption to concentration. The measured rate constant for the self-reaction at room temperature is approximately a factor of 2 lower than literature recommendations. The reaction displays a slightly negative temperature dependence, which can be represented by a negative activation energy, $(E_a/R) = -400$ K. The laser absorption results are supported by independent experiments at 298 K and 4 Torr using time-resolved synchrotron-photoionization mass-spectrometric detection of the products of divinyl ketone and methyl vinyl ketone photolysis. The photoionization mass spectrometry experiments additionally show that methyl + propargyl are formed in the vinyl radical self-reaction, with an estimated branching fraction of 0.5 at 298 K and 4 Torr.

Introduction

Reactions of the vinyl radical (C_2H_3) are important in hydrocarbon combustion and planetary atmospheres. The self-reaction of vinyl,

$$C_2H_3 + C_2H_3 \rightarrow \text{products} \quad (1)$$

is a key reaction in all these systems. Reaction 1 can form 1,3-butadiene or bimolecular products:

$$C_2H_3 + C_2H_3 \rightarrow C_4H_6 \quad (1a)$$

$$C_2H_3 + C_2H_3 \rightarrow C_2H_4 + C_2H_2 \quad (1b)$$

$$C_2H_3 + C_2H_3 \rightarrow CH_3 + C_3H_3 \quad (1c)$$

The reaction at room temperature has been measured[1−4] to be substantially faster than would be expected from simple gas-kinetic considerations for recombination of two doublet radicals on the singlet surface, leading to the suggestion that the energetically accessible $^3B_{1u}$ state of 1,3-butadiene participates in the reaction.[4] Recently, measurements of the vinyl radical visible absorption cross section that determined the vinyl radical concentration by photochemical means[5] were found to conflict with determinations that relied on kinetic decays and the literature value of k_1 to establish the vinyl concentration.[6] This led to the suggestion that the reported rate constant k_1 was significantly in error.[5]

The branching among the various product channels for the vinyl recombination has also been investigated. The low-pressure measurements of Thorn et al.[3] (1 Torr) and MacFadden and Currie[7] (<200 mTorr) showed essentially 100% branching to product 1b, but higher-pressure measurements by Fahr and co-workers[1,2,8] gave 1,3-butadiene as the dominant product. All of these experiments considered only 1a and 1b as viable channels; Thorn et al.[3] attempted to detect channel 1c but were unsuccessful. However, multiplexed mass spectrometric detection of products from photolysis of methyl vinyl ketone and divinyl ketone showed evidence of propargyl formation attributed to reaction 1c.[9,10]

The present study reinvestigates the kinetics of the vinyl radical self-reaction by two independent methods. A laser-photolysis/laser-absorption technique is employed, using 266 nm photolysis of vinyl iodide to generate vinyl and I atoms

* To whom correspondence should be addressed. E-mail: whgreen@mit.edu (W.H.G.), cataatj@sandia.gov (C.A.T.).

† Present address: Baker Petrolite, 12645 West Airport Blvd, Sugar Land, TX 77478-6120.

‡ Sandia National Laboratories Physical Sciences Institute intern.

§ Present address: Department of Chemical Engineering, The University of Texas at Austin, 1 University Station, Mail Code C0400, Austin, TX 78712-0231.

|| Present address: The Rockefeller University, 1230 York Avenue, Box 369, New York, NY 10065.

⊥ Present address: Department of Chemistry, University of San Francisco, 2130 Fulton St., San Francisco, CA 94117.

10.1021/jp8096132 CCC: $40.75
Published on Web 01/15/2009

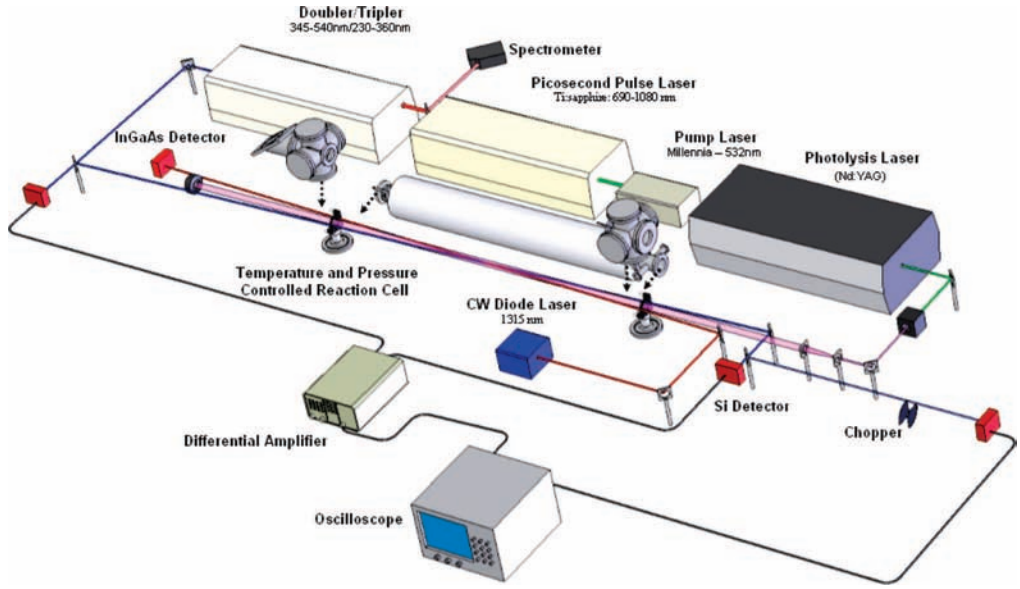

Figure 1. Diagram of the laser-photolysis/laser-absorption apparatus at MIT's CDL. The reactor and mirror housings are shown displaced from their actual locations (dotted arrows) to allow the laser paths to be seen. The apparatus at the CRF of Sandia National Laboratories is similar, except that a second CW diode laser is used for the visible absorption of the vinyl radical, in place of the tunable picosecond Ti:Al_2O_3 system.

concurrently.[11] Infrared laser absorption detection of I atoms in the $^2P_{1/2} \leftarrow {}^2P_{3/2}$ transition[12] is used to determine the initial concentration of I, and by extension, that of vinyl. The measured room-temperature rate coefficients at 20 Torr are ~ 50% of the literature recommendations. The temperature dependence of the reaction is also measured by this method. Furthermore, laser-photolysis/synchrotron-photoionization mass spectrometry[9,13] is used to measure time-resolved concentration profiles of photofragments and reaction products from the photolysis of divinyl ketone. The initial radical concentration is derived from the measured photolytic depletion of the known divinyl ketone concentration. Kinetic simulations reproduce the observed reactant, intermediate, and product profiles and yield a rate coefficient for vinyl self-reaction in excellent agreement with that determined by the laser absorption technique. The kinetic simulation also provides branching fractions for the individual reaction channels at 298 K and 4 Torr. The present results are irreconcilable with the reported results of Thorn et al.,[3] but the possibility that stabilization of triplet 1,3-butadiene is responsible for the discrepancy with the higher-pressure (100−400 Torr) results of Fahr and co-workers[1,2,4] cannot be excluded.

Experiment

The measurements of the vinyl radical self-reaction were carried out using two independent methods in three different laboratories. Laser-photolysis/laser-absorption experiments were undertaken both in the Combustion Dynamics Laboratory (CDL) at the Massachusetts Institute of Technology (MIT) and in the Combustion Research Facility (CRF) at Sandia National Laboratories. Further experiments were conducted using the Multiplexed Chemical Kinetics Reactor[13−16] that operates on the Chemical Dynamics Beamline of the Advanced Light Source (ALS) of the Lawrence Berkeley National Laboratory.

Laser Absorption Measurements. The methods used for laser photolysis/laser absorption measurements are similar to those employed in earlier publications.[5,17−19] The experimental apparatus is represented in Figure 1. The MIT apparatus is as described elsewhere,[18,19] with the addition of a narrow linewidth, low-noise continuous-wave (CW) diode laser tuned to the ($F = 3\ ^2P_{1/2} \leftarrow F = 2\ ^2P_{3/2}$) I atom atomic transition. The vinyl radical is produced by 266 nm photolysis of vinyl iodide, which produces essentially exclusively I + C_2H_3 fragments.[11] The vinyl radical concentration is monitored via multiple pass absorption in the $\tilde{A} \leftarrow \tilde{X}$ band,[6,20−22] using a CW diode laser near 404 nm (Sandia)[5] or the doubled output of a mode-locked Ti:Al_2O_3 laser (1.2 ps at 80 MHz) at one of three absorption bands, 404 nm, 423.2 nm, or 445.0 nm (MIT).[18] A high resolution (0.1 nm full width at half-maximum (fwhm)) spectrometer was used to determine the output wavelength of the Ti:Al_2O_3 probe laser. In both instruments, the sensitivity of the vinyl radical measurement is enhanced with a Herriott-type multipass resonator[23] that gives an absorption path length of up to 40 m. The experiments were carried out in a 160 cm temperature-controlled stainless steel (MIT) or quartz (Sandia) flow reactor. The precision of temperature control in the probed region of the reactor is typically better than 1%.[23] The flows of reactant and buffer gases were regulated by calibrated mass flow controllers, and the internal pressure of the reactor was monitored by a capacitance manometer and controlled via an automated butterfly valve. The temperature was controlled by a cylindrical oven around the center of the reactor and additional resistive heaters near the reactor entrance and exit. Three K-type thermocouples provided feedback to microprocessors that controlled the heater current.

The initial vinyl radical concentrations were taken to be equal to the initial concentration of I atoms ($[I]_0$) produced by the photolysis pulse.[11] An external-cavity diode laser, passed once through the reactor, was used to probe the I atom ($F = 3\ ^2P_{1/2} \leftarrow F = 4\ ^2P_{3/2}$) transition at 1315.28 nm. The I atoms produced from vinyl iodide photolysis are formed in both the ground state ($^2P_{3/2}$) and the excited spin−orbit state ($^2P_{1/2}$, denoted I*). Two different methods were employed to determine the total initial iodine atom concentration $[I]_0$. In the first method, O_2 or C_2H_4 was used to quench I($^2P_{1/2}$) to the ground state. Enough quencher was used so that quenching was much more rapid than reactive I loss channels. Oxygen, however, reacts very quickly with vinyl, preventing simultaneous measurement of vinyl radical kinetics. Therefore, when quenching with O_2, time traces for vinyl and I-atom were acquired in back-to-back measurements. Fluctuations in flow conditions and photolysis power might contribute to the uncertainty in this method to determine $[I]_0$. Therefore,

in some cases, C_2H_4 was used as an alternative quencher, because it reacts with vinyl much more slowly at room temperature than does oxygen;[18] however, it is also a much less effective quencher. The second method uses a determination of the I spin−orbit branching ratio (Φ_{I^*}) for vinyl iodide photolysis, defined as $[I(^2P_{1/2})]_0/([I(^2P_{3/2})]_0 + [I(^2P_{1/2})]_0)$. The advantage of this method is that the time traces for vinyl and I atom can be acquired simultaneously. The spin−orbit branching is measured by the absorption-versus-gain procedure developed by Leone and co-workers.[24−26] From the initial value of the transient absorption on the I-atom transition, denoted A_0, and Φ_{I^*}, one can determine $[I]_0$ via the equation

$$\sigma_I[I]_0 = \frac{-A_0}{3\Phi_{I^*} - 1} \quad (2)$$

The major source of error in this method is from the determination of Φ_{I^*}. Unquenched and quenched I-atom absorption traces were taken in every experiment; therefore both methods were applied to every trace. Additionally, at MIT experiments were performed for various concentrations of vinyl iodide, at different photolysis pulse energies, for different diameters of the photolysis beam, and at three different vinyl probe wavelengths.

In the experiments at MIT, vinyl radicals were detected by multiple-pass laser absorption at one of three absorption bands, 404 nm, 423.2 nm, and 445.0.[27] Multiple absorption lines were used to eliminate possible systematic error from background absorption by a product species. The concentration of vinyl iodide was varied from 0.9×10^{15} to 6.4×10^{15} molecules cm^{-3}, which yielded vinyl radical concentration ranging from 0.5×10^{13} to 1.0×10^{13} molecules cm^{-3}. Photolysis power was varied from 11 to 32 mJ/pulse in order to verify that no competing photochemical effects were being observed. Measurements were made at two photolysis beam diameters, 1.25 and 1.75 cm, in order to verify the accuracy of the measured spatial overlap of the probe and photolysis beams. The combined variations in photolysis power, power density, and precursor concentrations gave initial vinyl concentrations of $(0.16-4.5) \times 10^{13}$ cm^{-3}.

To determine k_1, the time-dependent vinyl absorption signal is normalized to 1 and fitted to second-order decay:

$$\frac{[C_2H_3]_t}{[C_2H_3]_0} = \frac{1}{1 + 2k't} \quad (3)$$

where $k' = k_1[C_2H_3]_0$. In principle, this second-order rate constant, k', could include contributions from $C_2H_3 + I \rightarrow C_2H_3I$. However, C_2H_3 decays on a submillisecond time scale, while the I atom persists for >5 ms, indicating that the reaction of $C_2H_3 + I$ is much slower than that of $C_2H_3 + C_2H_3$.[5] At sufficiently high vinyl radical concentrations, removal by self-reaction dominates over competing loss channels such as diffusion out of the beam path or reaction with impurities. Dividing k' by $[I]_0$ then yields the true rate coefficient k_1, under the assumption that $[C_2H_3]_0 = [I]_0$.[11] A typical transient absorption signal of vinyl radical and the second-order fit with residuals are shown in Figure 2.

Photoionization Mass Spectrometry Measurements. The Multiplexed Chemical Kinetics Reactor has been described in other publications;[13−16] reactions are initiated by laser photolysis of a suitable precursor in a quartz slow-flow reactor. In the present measurements, 193 or 248 nm photolysis of divinyl ketone (pentadien-3-one) or 193 nm photolysis of methyl vinyl ketone (but-3-en-2-one) is used to generate vinyl radicals. The contents of the reactor are continuously sampled via a small

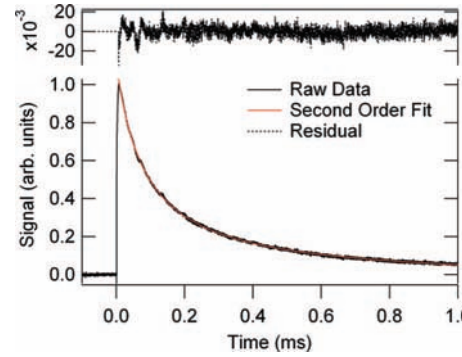

Figure 2. Transient absorption signal for vinyl radical. The second order fit to the decay is shown as a red line, with the corresponding residuals shown on top.

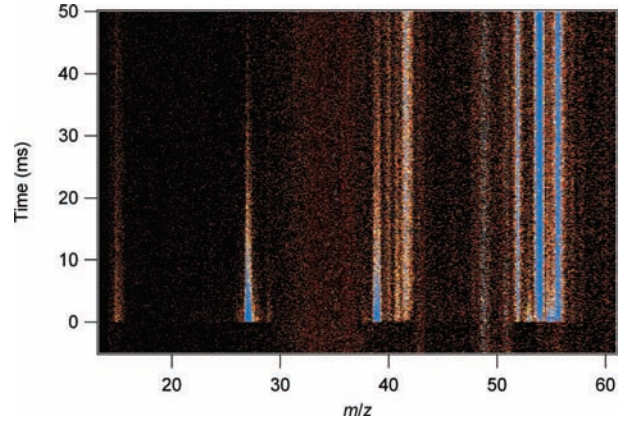

Figure 3. Section of the time-resolved mass spectrum following 193 nm photolysis of divinyl ketone, taken with 10.2 eV photoionization.

(~600 μm) hole in the side of the quartz tube. The nearly effusive beam is probed by photoionization mass spectrometry, using tunable vacuum ultraviolet radiation from the Chemical Dynamics Beamline at the ALS at Lawrence Berkeley National Laboratory. After ionization by the synchrotron beam, ions are analyzed by a Mattauch−Herzog double-focusing mass spectrometer, and each ion is detected on a time- and position-sensitive detector. Each ion detected is labeled by its position (related to its m/z) and the time of arrival relative to the photolysis pulse.[13] A histogram of these events gives a two-dimensional image of the evolving mass spectrum as a function of time relative to the photolysis. The double-focusing mass spectrometer detects all species over an m/z range of a factor of up to approximately 8. Vinyl iodide photolysis proved less practical than photolysis of the ketones, in part because of the difficulty in detecting all relevant species (including methyl radical) together with the precursor ($m/z = 154$). Figure 3 shows a typical image for the photolysis of divinyl ketone, taken with 10.2 eV photon energy. This energy is below the ionization energy of the ethane and acetylene products of vinyl radical disproportionation, but measurements at higher photon energy were made to probe that channel. The absolute photoionization efficiencies of vinyl, methyl, propargyl, and most of the stable reaction products are known;[10,28−30] with these cross sections and the initial radical concentration, absolute concentration-versus-time profiles can be constructed. The derivation of the initial radical concentration is subject to several sources of uncertainty. It is derived similarly to other work on radical−radical reactions, by measuring the depletion of the precursor by the photolysis laser.[31] If the yield of photolysis products is known, this gives the initial radical concentration as a proportion of

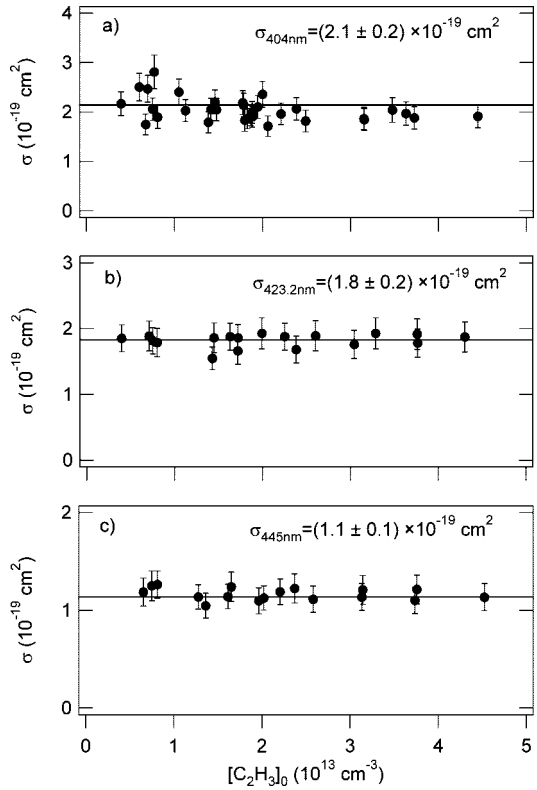

Figure 4. Plots of the vinyl radical absorption cross sections at 293 K and (a) 404 nm, (b) 423.2 nm, and (c) 445 nm as a function of initial vinyl concentration. The error bars are based on propagated ($\pm 1\sigma$) overall uncertainties.

the photolyte concentration. In the present experiments, the methyl vinyl ketone concentration is derived by calibrating the detection with known concentrations of hydrocarbon of a well-determined photoionization cross section,[29,30] and using the measured photoionization cross section of methyl vinyl ketone[10,32] to convert its signal to absolute concentration. The divinyl ketone photoionization cross section is not known; divinyl ketone is introduced by bubbling He through a liquid sample held in a temperature-controlled bath and sending a calibrated flow of the resulting (presumably saturated) mixture into the reactor. The vapor pressure of the divinyl ketone sample was measured directly, and the absolute divinyl ketone concentration was derived assuming that this was the partial pressure in the calibrated flow through the reactor. As divinyl ketone photolysis produces significant fractions of other reactive species besides vinyl radicals, rate coefficients are determined from kinetic simulations.

Results

Vinyl Radical Absorption Cross Section. Using direct absorption by I atom to determine the initial radical concentration, the vinyl radical absorption cross sections were determined at three different probe wavelengths. The cross-section σ_{vinyl} is given by Beer's law:

$$\sigma_{vinyl} = \frac{-A_{C_2H_3}}{[I]_0 \times l} \quad (4)$$

where l is the path length for probe laser for vinyl radical, $A_{C_2H_3}$ is the peak base e absorbance ($A = -\ln(I/I_0)$) of the probe laser, and $[I]_0 = [C_2H_3]_0$ is the initial concentration of I atoms. The results from the current study are summarized in Figure 4, where

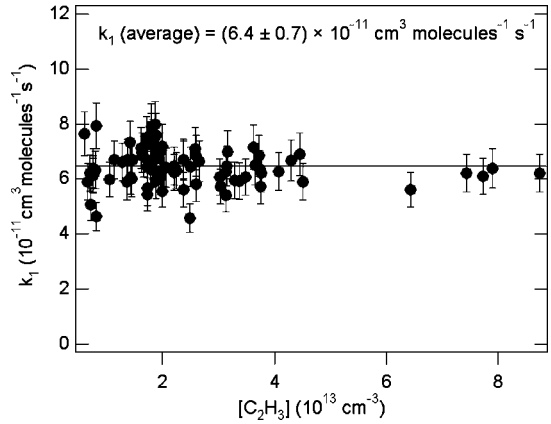

Figure 5. Measured rate constant (293 K) for the self-reaction of vinyl radical at various initial vinyl concentrations. The error bars are based on ($\pm 1\sigma$) propagated random uncertainty and do not include the systematic uncertainty in the iodine atom absorption cross section (see text for details).

σ_{vinyl} is shown versus $[C_2H_3]_0$. The photolysis power, photolysis diameter, and vinyl iodide concentration were varied to determine the reproducibility and consistency of σ_{vinyl}. The average cross-sections determined from all these measurements are

$$\sigma_{404} = (2.1 \pm 0.4) \times 10^{-19}\ \text{cm}^2 \quad (5)$$

$$\sigma_{423.2} = (1.8 \pm 0.4) \times 10^{-19}\ \text{cm}^2 \quad (6)$$

$$\sigma_{445} = (1.1 \pm 0.2) \times 10^{-19}\ \text{cm}^2 \quad (7)$$

The error reported is $\pm 2\sigma$ standard deviation. Several authors have published values of σ_{404} and σ_{445} in the literature. Recently, DeSain et al.[5] reported $\sigma_{404} = (2.9 \pm 0.4) \times 10^{-19}$ cm^2. The MIT results show the cross section for the 404 nm band to be slightly (~40%) smaller than the determinations at the CRF.[5] This discrepancy may arise in part from differences in the frequency spectra of the probe lasers used. Because the initial radical concentration for the kinetics is derived from the I atom signal, the difference in the derived absorption cross section does not affect the rate coefficient determinations. The σ_{445} was estimated by Hunziker et al.[22] to be 0.8×10^{-19} cm^2, whereas Tonokura et al.[6] reported $\sigma_{445} = 4.9 \times 10^{-19}$ cm^2. The present results agree very well with Hunziker et al.[22] but are in substantial disagreement with the results of Tonokura. However, Tonokura et al.[6] determined the vinyl concentrations on the basis of the self-reaction rate coefficient, which the present work considerably revises.

Vinyl + Vinyl Rate Coefficient. To determine the self-reaction rate constant for vinyl radical (k_1), two methods were used to determine $[C_2H_3]_0$. A summary of the MIT determinations of k_1 versus $[C_2H_3]_0$ at room temperature is shown in Figure 5. The mean k_1 at 293 K is

$$k_1 = (6.4 \pm 2.2) \times 10^{-11}\ \text{cm}^3\ \text{molecule}^{-1}\ \text{s}^{-1} \quad (8)$$

The error limits are $\pm 2\sigma$ on the basis of the statistical uncertainties convolved with the uncertainty in the I atom cross section, σ_I, which is the primary source of uncertainty in determining k_1. Ha et al.[12] report 95% confidence limits of approximately ±24% for the integrated line strength for the $^2P_{1/2} \leftarrow {}^2P_{3/2}$ transition of the I atom, which is the predominant uncertainty in σ_I, and hence in k_1. The combined effect of Doppler and pressure broadening effects upon the I atom absorption line is given by the Voigt profile. The half-width of the Voigt profile is calculated according to the approximation

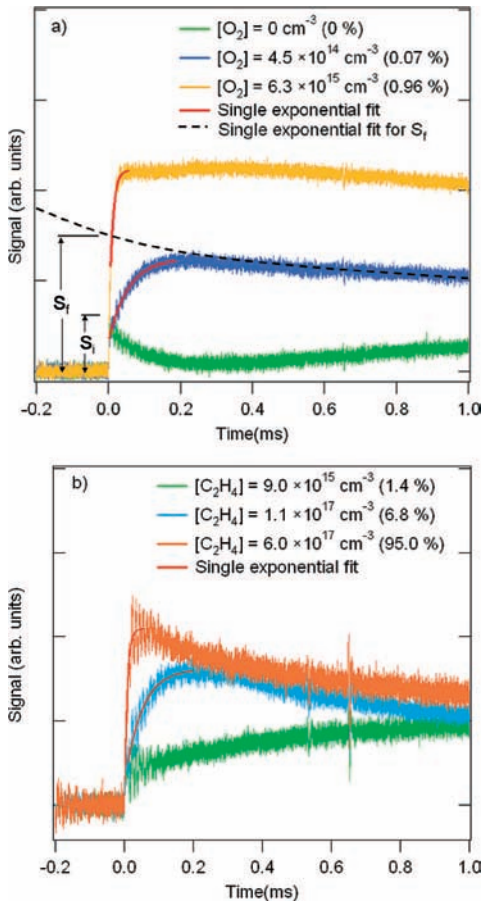

Figure 6. Transient absorption signal for I atom at 1315.14 nm upon photolysis of vinyl iodide at 266 nm. A prompt absorption is observed on the 1315.14 nm probe laser. The I($^2P_{1/2}$) atoms are quenched by (a) O_2 or (b) C_2H_4 on a short time scale to yield ground-state iodine atoms. The I($^2P_{3/2}$) population is removed via diffusion and recombination processes. The initial (S_i) and final absorption (S_f) are obtained via back-extrapolation based on a single exponential fit (solid and dashed lines).

described by Whiting,[33] an approximation that involves a negligible error of ~3%. Including uncertainties in the temperature-dependent collision-broadening parameters from Davis et al.[34] gives an overall propagated uncertainty of approximately ±27% (2σ) in σ_I.

As described above, two different methods were used to determine initial vinyl concentration, $[C_2H_3]_0$. The first method, using added O_2 or C_2H_4 to quench I($^2P_{1/2}$), is illustrated in Figure 6. The prompt decay immediately after the photolysis pulse occurs from the balance between stimulated emission from the excited ($^2P_{1/2}$) state and absorption from the ground ($^2P_{3/2}$) state for the I atoms. The second decay after the prompt decay occurs as a result of the quenching of excited I($^2P_{1/2}$) atoms to ground-state I atoms by collisions with the bath gas. Oxygen is a much more efficient quencher than C_2H_4, so much higher $[C_2H_4]$ is required to effectively quench the I($^2P_{1/2}$) atoms. By assuming pseudo-first-order kinetics and fitting the second decay to a single exponential, quenching rates of I($^2P_{1/2}$) by O_2 and C_2H_4 can be determined. The measured I($^2P_{1/2}$) quenching rate by O_2 is $(2.8 \pm 0.1) \times 10^{-11}$ cm^3 molecule^{-1} s^{-1}, which agrees very well with literature determinations.[35−37] The rate constant for quenching of I($^2P_{1/2}$) by C_2H_4 is measured to be $(1.9 \pm 0.1) \times 10^{-14}$ cm^3 molecule^{-1} s^{-1}, approximately a factor of 10 smaller than the value from Deakin and Husain,[36,37] perhaps suggesting quenching by impurities in the earlier work.

Under the present experimental conditions, 0.5−1.0% O_2 was found to be optimal to rapidly quench I($^2P_{1/2}$) → I($^2P_{3/2}$) and determine $[I]_0$. Above O_2 mole fractions of about 1.0%, a third decay was observed in the transient absorption of I atom, which might arise from secondary I atom production from O_2 reactions. In this method, an additional source of uncertainty could come from flow and photolysis pulse fluctuation between the experiments to vinyl time dependence and initial I atom concentration. These uncertainties are much smaller than that in the I absorption cross section. Combining the 15−20% random uncertainties with the uncertainty in σ_I yields a net propagated $\pm 2\sigma$ uncertainty of 30−35% in k_1. The $[C_2H_3]_0$ determined using this method gives the k_1 value reported as eq 8. The optimal C_2H_4 mole fraction for quenching was found to be between 40−95%. With C_2H_4 as a quenching gas, transient absorption of vinyl radical and I atom could be taken simultaneously, but high $[C_2H_4]$ also led to thermal lensing in the vinyl absorption signal. As shown in Figure 6b, the acoustic noise in the transient I signal, leads to additional uncertainty in $[I]_0$. The two quenching gases led to similar k_1 values, but the propagated $\pm 2\sigma$ error due to acoustic noise and thermal lensing in the C_2H_4 case was substantial, making this a less-desirable technique for $[I]_0$ determination.

The other method used to determine $[I]_0$ is via determination of the branching fraction of I($^2P_{1/2}$) formation (Φ_{I^*}). The advantage of this method is that simultaneous measurement of I atom and vinyl signal avoids uncertainty due to fluctuations in flow conditions and photolysis power. Using the method outlined by Leone and co-workers,[24,26] $\Phi_{I^*} = (0.25 \pm 0.03)$ is determined for vinyl iodide at 266 nm. These results are within the uncertainties of $\Phi_{I^*} = (0.27 \pm 0.01)$, reported by Zou et al.[11] Using the Φ_{I^*} from the present study gives $k_1(\Phi_{I^*} = 0.25) = (6.7 \pm 3.8) \times 10^{-11}$ cm^3 molecule^{-1} s^{-1}. The ~60% ($\pm 2\sigma$) uncertainty in $k_1(\Phi_{I^*} = 0.25)$ comes from the uncertainty in the present determination of Φ_{I^*} (as can be seen from eq 2, the uncertainty in Φ_{I^*} becomes dramatically more important near the degeneracy point $\Phi_{I^*} = 1/3$). Using the Φ_{I^*} from Zou et al.[11] would yield a slightly smaller rate constant of $k_1(\Phi_{I^*} = 0.27) = (5.5 \pm 1.7) \times 10^{-11}$ cm^3 molecule^{-1} s^{-1}. In all of the MIT experiments, the self-reaction rate constant is essentially the same (within 15%), regardless of the method used to analyze the signal; the only difference is the size of the error bounds. As the 1% oxygen method yields smaller uncertainties, this method is employed to determine $[I]_0$, and the k_1 determined from this method is therefore reported as the recommended value.

The determinations of the temperature dependence of the rate coefficient are made from measurements at the CRF of Sandia National Laboratories. The rate constant exhibits a slight negative temperature dependence, shown in Figure 7, as is typical for barrierless radical−radical recombination. The temperature dependence is adequately described by

$$k_1 = 1.2 \times 10^{-11} \text{ cm}^3 \text{ molecule}^{-1} \text{ s}^{-1} e^{(+400/T)} \qquad (9)$$

The CRF measurements display the same internal consistency between the two methods of $[I]_0$ determination as do the MIT measurements. The CRF determination gives a slightly smaller rate coefficient at room temperature (298 K), $k_1 = (5.1 \pm 1.5) \times 10^{-11}$ cm^3 molecule^{-1} s^{-1}. Although the measurements agree to within their absolute $\pm 2\sigma$ uncertainty estimates, these uncertainties are dominated by the uncertainty in σ_I, on which both determinations rely; the relative uncertainty is therefore much smaller. The overlap path length is measured in an identical fashion in both laboratories. Partial saturation of the

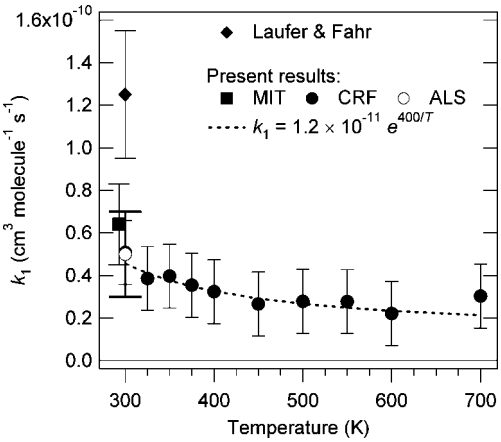

Figure 7. Plot of the rate coefficient for vinyl radical self-reaction, k_1. The measurements from the CRF are shown as the filled circles, that from the photoionization mass spectrometric measurements at the ALS is shown as the open circle, and that from the CDL at MIT is shown as the filled square. The rate constant recommended by the Laufer and Fahr review[4] is shown for comparison.

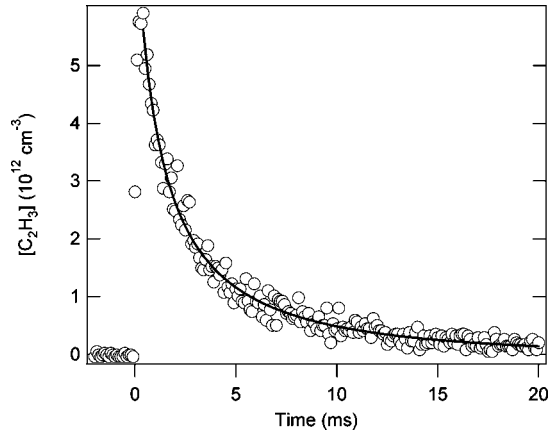

Figure 8. Time-dependent vinyl radical concentration observed following the photolysis of divinyl ketone at 193 nm. The solid line is a fit to a combined first- and second-order decay, which gives $k' \equiv ([C_2H_3]_0\ k_1) = (380 \pm 40)\ s^{-1}$. The absolute concentration axis is determined from the measured depletion of the precursor, combined with an analysis of photoproduct yields from the observed mass spectra (see text and Table 1).

I-atom detectors could lead to an apparent absorption smaller than the real absorption, which would give an erroneously small estimate of the initial vinyl concentration (and hence an erroneously large k_1). The incident power is somewhat larger in the MIT experiments; however, the detectors were carefully maintained in the linear regime in both laboratories. The initial concentration derived in the MIT experiments is in closer agreement with an estimate based on the concentration of vinyl iodide, the incident 266 nm power, and the vinyl iodide absorption cross section, assuming a unity photodissociation quantum yield; however, the uncertainties of such a determination exceed the disagreement between the two laboratories. Other possible sources of systematic error, e.g., in the frequency of the I atom absorption laser, in the photolysis laser profile, or in the cross-section calculations, have been investigated and similarly discounted. The source of the difference in rate constant determination between the two laboratories is not clear.

Product Measurements. The mass spectrum from 193 nm divinyl ketone (DVK) photolysis and subsequent reactions of the photofragments is shown in Figure 3. The individual mass channels can be integrated to give a time-resolved relative concentration of each species,[9,13] which can be put on an absolute scale by measuring the depletion of the known concentration of the photolyte.[10,31] The time-resolved vinyl radical signal from 193 nm photolysis of divinyl ketone is shown in Figure 8. A fit of this trace to a combined first- and second-order decay[38] is shown as the solid line. The measured photolytic depletion of divinyl ketone in this trace is $\Delta(\mathrm{DVK}) = -5.3 \times 10^{12}\ \mathrm{cm}^{-3}$. If the photolysis produced solely 2 C_2H_3 + CO (i.e., $[C_2H_3]_0 = 1.1 \times 10^{13}\ \mathrm{cm}^{-3}$), the derived second-order rate coefficient would be $k_1 \sim 3.6 \times 10^{-11}\ \mathrm{cm}^3\ \mathrm{molecule}^{-1}\ \mathrm{s}^{-1}$; however, as visible in Figure 3, other photolysis channels are significant. The known absolute cross sections for CH_3, C_2H_3, propargyl, propene, butadiene, ethene, and so forth allow the relative concentrations of all these species to be established, with absolute concentrations given by a single overall scaling factor fixed by the condition $\Delta(\mathrm{DVK}) = -5.3 \times 10^{12}\ \mathrm{cm}^{-3}$. In practice, this requires some assumptions to be made about the photolysis channels that produce various fragments,[31] as some photoproducts with high ionization energies are not detected (e.g., C_2H_2 or CO).

Figure 9 shows derived absolute concentration profiles for a number of photofragments and reaction products from divinyl ketone photolysis. The dominant photolysis channel observed is indeed 2 C_2H_3 + CO; however, the time traces of propargyl and $m/z = 54$ (which may include contributions from CH_2CCO) cannot be fit satisfactorily without assuming some direct photolytic production. The solid lines in Figure 9 reflect a kinetic simulation[39] based on the mechanism given in Table 1. This simulation yields a second-order rate coefficient for vinyl radical self-reaction of $5 \times 10^{-11}\ \mathrm{cm}^3\ \mathrm{molecule}^{-1}\ \mathrm{s}^{-1}$, under the assumption that no observed photofragment is produced in conjunction with any other. That is to say, the derived initial vinyl radical concentration is reduced from its maximum, $[C_2H_3]_0 = -2\ \Delta(\mathrm{DVK})$, by twice the sum of the concentrations of other observed prompt photofragments. This assumption could systematically overestimate the rate coefficient if, for example, a photolysis channel that produces CH_2CCO also produces vinyl; however, this is countered by the possibility that some photolysis channels remain unobserved. An overall uncertainty of ± 40%, including uncertainty in the initial divinyl ketone concentration, the second-order component of the vinyl decay, and the photolysis yield, is assigned to the k_1 determination by this method, giving

$$k_1 = (5 \pm 2) \times 10^{-11}\ \mathrm{cm}^3\ \mathrm{molecule}^{-1}\ \mathrm{s}^{-1} \qquad (10)$$

A clear production of methyl and propargyl radicals is observed from the vinyl radical self-reaction; the simulation with a branching fraction of 0.5, shown in Figure 9, fits the concentration profiles of both species. Furthermore, the same mechanism fits concentration profiles observed from 193 nm methyl vinyl ketone photolysis (Figure 10). Simulations of the ethene product and of the secondary products allyl (from vinyl + methyl), propene (from vinyl + methyl), and butene (from methyl + allyl) are in similar agreement, and are shown in Figures S1−S3 of the Supporting Information. Products of the vinyl + propargyl reaction at $m/z = 66$ (C_5H_6) and the vinyl + allyl reaction at $m/z = 68$ (C_5H_8) are also detected, with a time dependence that matches the model predictions. The cross sections for these species have not been measured, precluding quantitative comparison, but scaling the observed signal using the cross-section estimation method of Bobeldijk et al.[40] yields good agreement with the kinetic model (shown in Figure S4 of the Supporting Information). A simplified integrated-profiles[41,42] method can also be used to derive k_1 from the methyl vinyl ketone measurements, without prior knowledge of the initial

TABLE 1: Kinetic Mechanism Used to Model the Photoionization Mass-Spectrometric Measurements of 193 nm Divinyl Ketone Photolysis at 298 K and 4 Torr

reaction	rate coefficient	reference
$C_2H_3 + C_2H_3 \rightarrow$ products (k_1)	5.0×10^{-11} cm^3 molecule^{-1} s^{-1}	present work
(k_{1a}/k_1)	0.2	present work
(k_{1b}/k_1)	0.3	present work
(k_{1c}/k_1)	0.5	present work
$CH_3 + C_2H_3 \rightarrow$ products	1.2×10^{-10} cm^3 molecule^{-1} s^{-1}	45
$CH_3 + C_2H_3 \rightarrow C_3H_5 + H$	$\Phi = 0.15$	45
$CH_3 + C_2H_3 \rightarrow C_3H_6$	$\Phi = 0.45$[a]	45
$CH_3 + CH_3 \rightarrow C_2H_6$ (at 4 Torr He)	3.7×10^{-11} cm^3 molecule^{-1} s^{-1}	46
$C_3H_3 + C_3H_3 \rightarrow$ products	3.9×10^{-11} cm^3 molecule^{-1} s^{-1}	53
$CH_3 + C_3H_3 \rightarrow$ products	1.05×10^{-10} cm^3 molecule^{-1} s^{-1}	54
$C_3H_3 + C_2H_3 \rightarrow C_5H_6$	4.0×10^{-11} cm^3 molecule^{-1} s^{-1}	estimate
$C_3H_5 + CH_3 \rightarrow C_4H_8$	4.0×10^{-11} cm^3 molecule^{-1} s^{-1}	54
$C_3H_5 + C_2H_3 \rightarrow C_5H_8$	4.0×10^{-11} cm^3 molecule^{-1} s^{-1}	estimate
$H + C_2H_3 \rightarrow$ products	1.8×10^{-10} cm^3 molecule^{-1} s^{-1}	4
$H + C_3H_3 \rightarrow$ products	2.5×10^{-10} cm^3 molecule^{-1} s^{-1}	55
$H + C_3H_5 \rightarrow$ products	2.8×10^{-10} cm^3 molecule^{-1} s^{-1}	56
photolysis channel	**branching fraction**	**reference**
$C_2H_3C(O)C_2H_3 + h\nu \rightarrow 2\ C_2H_3 + CO$	0.67	present work
$C_2H_3C(O)C_2H_3 + h\nu \rightarrow C_3H_3 + ?$	0.13	present work
$C_2H_3C(O)C_2H_3 + h\nu \rightarrow C_2H_4 + ?$	0.13	present work
$C_2H_3C(O)C_2H_3 + h\nu \rightarrow m/z = 54 + ?$	0.07	present work

[a] Branching fraction into the specific product channel.

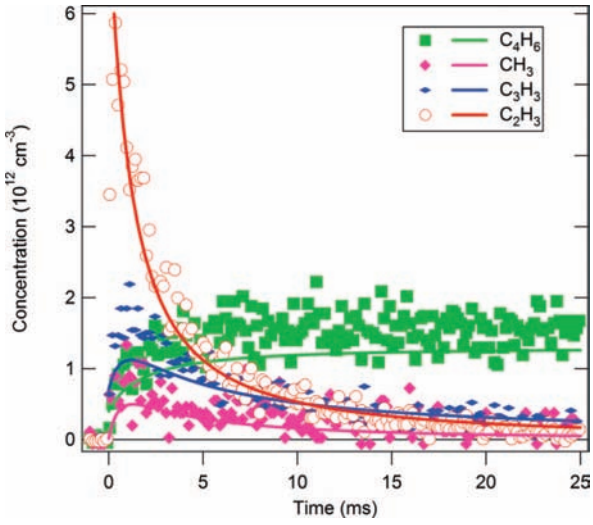

Figure 9. Absolute concentration profiles for several products following photolysis of divinyl ketone at 193 nm. The symbols are experimental data (markers on every third point), and the solid lines are simulations from the kinetic mechanism in Table 1.

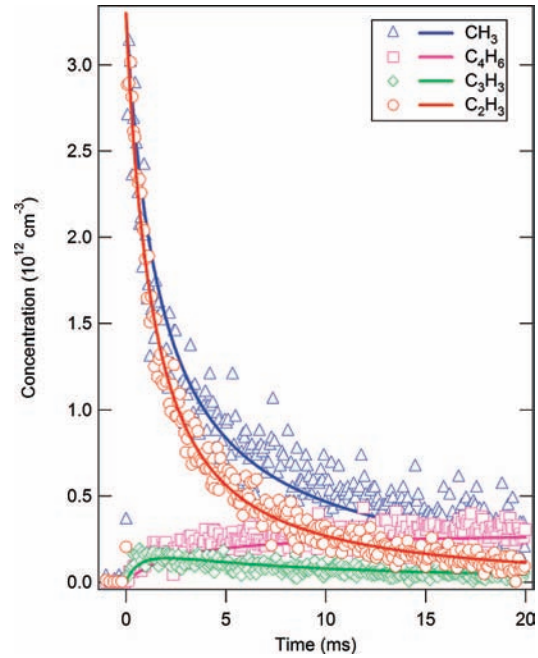

Figure 10. Absolute concentration profiles for several products following photolysis of methyl vinyl ketone at 193 nm. The symbols are experimental data (markers on every third point), and the solid lines are simulations from the kinetic mechanism in Table 1.

radical concentration. A derivation of this method is given in the Supporting Information; this analysis would yield $k_1 \sim 4.4 \times 10^{-11}$ cm^3 molecule^{-1} s^{-1}.

Uncertainty in the absolute photoionization cross sections of the radical species is approximately ±20−30%, and that of the stable species on the order of ±10−15%, so the agreement in amplitudes between the calculation and the experiment is within the uncertainty of the measurement. The branching fractions are estimated to be accurate to ±0.1. The measured branching fraction for C_2H_4 production is approximately 0.3, yielding a rate coefficient for disproportionation to $C_2H_4 + C_2H_2$ of

$$k_{1b} \sim (0.3 \times 5) \times 10^{-11}\ \text{cm}^3\ \text{molecule}^{-1}\ \text{s}^{-1} = 1.5 \times 10^{-11}\ \text{cm}^3\ \text{molecule}^{-1}\ \text{s}^{-1} \quad (11)$$

which, interestingly, is in excellent agreement with the specific rate constant for C_2H_4 production reported by Fahr and Laufer,[2] $k_{1b} = 1.8 \times 10^{-11}$ cm^3 molecule^{-1} s^{-1}.

Discussion

The kinetics of the vinyl + vinyl reaction have been previously investigated by several authors,[1−5,7,43] and the results from these studies are summarized in Table 2. MacFadden and Currie[7] measured k_1 to be 5.3×10^{-12} cm^3 molecule^{-1} s^{-1} at low pressures (≤200 mTorr) using flash photolysis of divinyl ether with time-of-flight mass spectrometric detection. Tsang and Hampson[43] estimated k_1 based on thermochemical considerations to be 1.76×10^{-11} cm^3 molecule^{-1} s^{-1}. Employing a discharge-flow/mass spectrometry technique, Thorn et al.[3] determined $k_1 = (1.4 \pm 0.6) \times 10^{-10}$ cm^3 molecule^{-1} s^{-1} at 298 K and 1 Torr. Fahr and Laufer[2] measured the room-temperature self-reaction rate constant at 400 Torr to be $k_1 =$

TABLE 2: Comparison of Room-Temperature Rate Constants for Vinyl Radical Self-Reaction from Literature and the Current Study

	method	pressure	k_1 (cm^3 $molecule^{-1}$ s^{-1})
MacFadden & Currie[7](1972)	time-of-flight mass spectrometry	65−200 mTorr	$(5.3 \pm 0.5) \times 10^{-12}$
Tsang & Hampson[43](1986)	thermochemical analysis		1.76×10^{-11}
Fahr & Laufer[1](1990)	flash photolysis/VUV absorption	400 Torr	$(1.0 \pm 0.25) \times 10^{-10}$
Thorn et al.[3](1996)	discharge-flow/mass spectrometer	1 Torr	$(1.41 \pm 0.60) \times 10^{-10}$
Laufer & Fahr[4](2004)	review		$(1.25 \pm 0.3) \times 10^{-10}$
DeSain et al.[5]	laser photolysis/laser absorption	20 Torr	$(4 \pm 2) \times 10^{-11}$
present study	laser photolysis/laser absorption	20 Torr	$(6.4 \pm 2.2) \times 10^{-11}$ (MIT) $(5.1 \pm 1.5) \times 10^{-11}$; 1.2×10^{-11} $e^{(+400\ K/T)}$ (CRF)
	laser photolysis/photoionization mass spectrometry	4 Torr	$(5 \pm 2) \times 10^{-11}$ (ALS)

$(1.0 \pm 0.25) \times 10^{-10}$ cm^3 $molecule^{-1}$ s^{-1} using a laser photolysis/vacuum ultraviolet absorption method, and Fahr et al.[1] employed similar techniques to derive a value of $k_1 = (1.3 \pm 0.14) \times 10^{-10}$ cm^3 $molecule^{-1}$ s^{-1} at 100 Torr. The recent review by Laufer and Fahr[4] recommends $k_1 = (1.25 \pm 0.3) \times 10^{-10}$ cm^3 $molecule^{-1}$ s^{-1}. In a preliminary determination using the laser photolysis/laser absorption technique, DeSain et al.[5] reported $k_1 = (4 \pm 2) \times 10^{-11}$ cm^3 $molecule^{-1}$ s^{-1} at 20 Torr. The present results for the vinyl radical self-reaction rate coefficient are in reasonable agreement with those of DeSain et al.[5] and are a factor of 2 or more lower than the results of Thorn et al.[3] and the recommendation of Laufer and Fahr.[4]

The rate coefficients reported by Fahr and co-workers[1,2,4] are unusually large for a radical recombination,[44] a difference that Laufer and Fahr[4] suggested could be due to the formation of triplet butadiene. For simple recombination, the geometric mean rule,

$$k_{(A+B)} = 2(k_{(A+A)} \times k_{(B+B)})^{1/2} \qquad (12)$$

which has been explicitly validated against alkyl + alkyl reactions,[44] can be used to evaluate k_1. The reaction of CH_3 with C_2H_3 has been independently determined by pseudo-first-order techniques, and the self-reaction of CH_3 radicals is well-characterized near room temperature. Using $k(CH_3 + C_2H_3) = (1.18 \pm 0.16) \times 10^{-10}$ cm^3 $molecule^{-1}$ s^{-1} from Stoliarov et al.[45] and the high-pressure limiting $k(CH_3 + CH_3)$ of $(5.9 \pm 0.2) \times 10^{-11}$ cm^3 $molecule^{-1}$ s^{-1} from Slagle et al.[46] would predict a value for k_1 of 5.9×10^{-11} cm^3 $molecule^{-1}$ s^{-1}, in close agreement with the present determinations. A slightly larger rate coefficient could be attributable to an independent direct disproportionation channel, a possibility supported by the similarity between the present k_{1b} and that derived by Fahr and Laufer.

The measurements of Fahr and co-workers,[1,2] carried out at higher pressure than the present experiments, derived the initial vinyl radical concentration from the butadiene yield and determined gas chromatographically, in combination with the branching ratio k_{1a}/k_{1b}. They observed only channels 1a and 1b in their experiments. One possible source of error in those determinations is therefore the branching ratio; if that ratio were substantially smaller, then the initial vinyl concentration would be larger, and hence the derived rate constant would be reduced. The photoionization measurements reported here show a substantial contribution from channel 1c, producing methyl and propargyl. However, this channel almost certainly arises from dissociation of a vibrationally excited 1,3-butadiene adduct formed in the initial encounter of the two vinyl radicals. Excited 1,3-butadiene can isomerize to 1,2-butadiene before dissociating, and thermal dissociation[47] and photolysis[48] of 1,3-butadiene both produce methyl + propargyl as the major products.[49] Increased stabilization of 1,3-butadiene at higher pressures would diminish the importance of channel 1c; it hence seems unlikely that this additional product channel is the sole source of the discrepancy between the present measurements and those of Fahr and co-workers.[1,2]

It is conceivable that the higher total rate coefficients observed at higher pressure simply reflect collisional stabilization. However, 193 nm photodissociation experiments by Robinson et al.[48] and the ab initio and Rice−Ramsperger−Kassel−Marcus (RRKM) calculations carried out by Lee et al.[49] on the C_4H_6 system indicate that the dissociation of 1,3-butadiene to two vinyl radicals is vastly disfavored relative to other bimolecular channels, even at 620 kJ mol^{-1} excess energy (i.e., about 150 kJ mol^{-1} above the vinyl + vinyl asymptote). Substantial back-dissociation from a 1,3-butadiene adduct in the vinyl + vinyl reaction is therefore exceedingly unlikely, all but ruling out any significant pressure dependence for recombination on the singlet surface. Nevertheless, the possibility of pressure-dependent recombination on the triplet surface, as suggested by Laufer and Fahr,[4] cannot be completely excluded.

The vertical excitation energy to the ^3B_u state of 1,3-butadiene has been measured to be 310 kJ mol^{-1} by electron energy-loss spectroscopy,[50] and the calculated adiabatic energy of the state from the symmetry adapted cluster configuration interaction (SAC-CI) method is 250 kJ mol^{-1}.[51] The ^3B_u state is therefore well below the energy of $C_2H_3 + C_2H_3$ which lies some 470 kJ mol^{-1} above the ground state of 1,3-butadiene.[49] If one assumes that the present experiments reflect a pressure-independent reaction on the singlet surface, then the discrepancy with the 400 Torr measurements[2] would be completely attributable to triplet reactions, with an overall rate coefficient of $\sim 5 \times 10^{-11}$ cm^3 $molecule^{-1}$ s^{-1}. (As the 100 Torr measurements of Fahr et al.[1] derived the absolute vinyl radical concentration assuming the same branching ratio as measured for 400 Torr, a decreased butadiene branching fraction would compensate for the lower rate coefficient and could give a similar apparent total rate constant to the 400 Torr measurements.) However, even a small barrier to reaction on the triplet surface could preclude it from making such a substantial contribution; the reaction of H + vinyl has a calculated barrier height of approximately 20 kJ mol^{-1}.[52] Computation of the triplet barrier to recombination and a reinvestigation of the rate coefficient at higher pressure (difficult with the large-volume reactors of the present experiments) may be required to firmly resolve the question of triplet participation in this reaction.

Conclusions

The recombination rate constant of vinyl radical has been studied as a function of temperature at a pressure of 20 Torr using laser-photolysis laser-absorption methods with vinyl iodide

as a precursor. Accurate determination of the initial radical concentration was obtained via direct laser absorption of I atom at 1315 nm. Vinyl radicals were probed at three different wavelengths: 404, 423.2, and 445 nm. Absorption cross sections (293 K) of the vinyl radical were measured to be $(2.1 \pm 0.4) \times 10^{-19}$ cm^2 at 404 nm, $(1.8 \pm 0.4) \times 10^{-19}$ cm^2 at 423.2 nm, and $(1.1 \pm 0.2) \times 10^{-19}$ cm^2 at 445 nm. The self-reaction rate constant for vinyl radical exhibits a slight negative temperature dependence, and its value at room temperature was found to be $(6.4 \pm 2.2) \times 10^{-11}$ cm^3 molecule^{-1} s^{-1} (293 K) in the MIT experiments and $(5.1 \pm 1.5) \times 10^{-11}$ cm^3 molecule^{-1} s^{-1} (298 K) in the CRF measurements. These results are ~50% lower than literature recommendations. Furthermore, completely independent measurements of time-resolved product concentrations following 193 nm photolysis of divinyl ketone and methyl vinyl ketone yield a self-reaction rate coefficient at 298 K and 4 Torr of $(5 \pm 2) \times 10^{-11}$ cm^3 molecule^{-1} s^{-1}, corroborating the laser-absorption determinations.

Acknowledgment. This work is supported by the Division of Chemical Sciences, Geosciences, and Biosciences, the Office of Basic Energy Sciences, the U.S. Department of Energy, with the work at MIT supported under contract DE-FG02-98ER14914. Sandia is a multiprogram laboratory operated by Sandia Corporation, a Lockheed Martin Company, for the National Nuclear Security Administration under contract DE-AC04-94-AL85000. Askar Fahr thanks NASA-Outer Planets Research Program for partial support of this work under Contract #NNX08AQ68G at Howard University. The Advanced Light Source is supported by the Director, Office of Science, Office of Basic Energy Sciences, Materials Sciences Division, of the U.S. Department of Energy under Contract No. DE-AC02-05CH11231 at Lawrence Berkeley National Laboratory. The Combustion Dynamics Laboratory thanks Professor R. W. Field (MIT) for lending the Nd:YAG laser used in this work, and the authors thank Darryl Sasaki (Sandia National Laboratories) for the synthesis of divinyl ketone.

Supporting Information Available: Comparison of model and experimental concentration profiles for ethene and secondary products from photodissociation of methyl vinyl ketone; integrated-profiles analysis of methyl vinyl ketone photolysis. This material is available free of charge via the Internet at http://pubs.acs.org.

References and Notes

(1) Fahr, A.; Laufer, A.; Klein, R.; Braun, W. *J. Phys. Chem.* **1991**, *95*, 3218.
(2) Fahr, A.; Laufer, A. H. *J. Phys. Chem.* **1990**, *94*, 726.
(3) Thorn, R. P.; Payne, W. A.; Stief, L. J.; Tardy, D. C. *J. Phys. Chem.* **1996**, *100*, 13594.
(4) Laufer, A. H.; Fahr, A. *Chem. Rev.* **2004**, *104*, 2813.
(5) DeSain, J. D.; Jusinski, L. E.; Taatjes, C. A. *Phys. Chem. Chem. Phys.* **2006**, *8*, 2240.
(6) Tonokura, K.; Marui, S.; Koshi, M. *Chem. Phys. Lett.* **1999**, *313*, 771.
(7) MacFadden, K. O.; Currie, C. L. *J. Chem. Phys.* **1973**, *58*, 1213.
(8) Fahr, A.; Braun, W.; Laufer, A. H. *J. Phys. Chem.* **1993**, *97*, 1502.
(9) Taatjes, C. A.; Hansen, N.; Osborn, D. L.; Kohse-Höinghaus, K.; Cool, T. A.; Westmoreland, P. R. *Phys. Chem. Chem. Phys.* **2008**, *10*, 20.
(10) Taatjes, C. A.; Meloni, G.; Selby, T. M.; Osborn, D. L.; Fan, H.; Pratt, S. T. *J. Phys. Chem. A* **2008**, *112*, 9336.
(11) Zou, P.; Strecker, K. E.; Ramirez-Serrano, J.; Jusinski, L. E.; Taatjes, C. A.; Osborn, D. L. *Phys. Chem. Chem. Phys.* **2008**, *10*, 713.
(12) Ha, T.-K.; He, Y.; Pochert, J.; Quack, M.; Ranz, R.; Seyfang, G.; Thanopoulos, I. *Ber. Bunsen-Ges. Phys. Chem.* **1995**, *99*, 384.
(13) Osborn, D. L.; Zou, P.; Johnsen, H.; Hayden, C. C.; Taatjes, C. A.; Knyazev, V. D.; North, S. W.; Peterka, D. S.; Ahmed, M.; Leone, S. R *Rev. Sci. Instrum.* **2008**, *79*, 104103.
(14) Meloni, G.; Zou, P.; Klippenstein, S. J.; Ahmed, M.; Leone, S. R.; Taatjes, C. A.; Osborn, D. L. *J. Am. Chem. Soc.* **2006**, *128*, 13559.
(15) Goulay, F.; Osborn, D. L.; Taatjes, C. A.; Zou, P.; Meloni, G.; Leone, S. R. *Phys. Chem. Chem. Phys.* **2007**, *9*, 4291.
(16) Meloni, G.; Selby, T. M.; Goulay, F.; Leone, S. R.; Osborn, D. L.; Taatjes, C. A. *J. Am. Chem. Soc.* **2007**, *129*, 14019.
(17) Striebel, F.; Jusinski, L. E.; Fahr, A.; Halpern, J. B.; Klippenstein, S. J.; Taatjes, C. A. *Phys. Chem. Chem. Phys.* **2004**, *6*, 2216.
(18) Ismail, H.; Goldsmith, C. F.; Abel, P. R.; Howe, P.-T.; Fahr, A.; Halpern, J. B.; Jusinski, L. E.; Georgievskii, Y.; Taatjes, C. A.; Green, W. H *J. Phys. Chem. A* **2007**, *111*, 6843.
(19) Goldsmith, C. F.; Ismail, H.; Abel, P. R.; Green, W. H. *Proc. Combust. Inst.* **2009**, *32*, 139–148.
(20) Pibel, C. D.; McIlroy, A.; Taatjes, C. A.; Alfred, S.; Patrick, K.; Halpern, J. B. *J. Chem. Phys.* **1999**, *110*, 1841.
(21) Pushkarsky, M. B.; Mann, A. M.; Yeston, J. S.; Moore, C. B. *J. Chem. Phys.* **2001**, *115*, 10738.
(22) Hunziker, H. E.; Kneppe, H.; McLean, A. D.; Siegbahn, P.; Wendt, H. R *Can. J. Chem.* **1983**, *61*, 993.
(23) Pilgrim, J. S.; Jennings, R. T.; Taatjes, C. A. *Rev. Sci. Instrum.* **1997**, *68*, 1875.
(24) Haugen, H. K.; Weitz, E.; Leone, S. R. *J. Chem. Phys.* **1985**, *83*, 3402.
(25) Hess, W. P.; Leone, S. R. *J. Chem. Phys.* **1986**, *86*, 3773.
(26) Hess, W. P.; Kohler, S. J.; Haugen, H. K.; Leone, S. R. *J. Chem. Phys.* **1986**, *84*, 2143.
(27) Shahu, M.; Yang, C.-H.; Pibel, C. D.; McIlroy, A.; Taatjes, C. A.; Halpern, J. B. *J. Chem. Phys.* **2002**, *116*, 8343.
(28) Robinson, J. C.; Sveum, N. E.; Neumark, D. M. *J. Chem. Phys.* **2003**, *119*, 5311.
(29) Cool, T. A.; Wang, J.; Nakajima, K.; Taatjes, C. A.; McIlroy, A. *Int. J. Mass. Spectrom.* **2005**, *247*, 18.
(30) Wang, J.; Yang, B.; Cool, T. A.; Hansen, N.; Kasper, T. *Int. J. Mass Spectrom.* **2008**, *269*, 210.
(31) Selby, T. M.; Meloni, G.; Goulay, F.; Leone, S. R.; Fahr, A.; Taatjes, C.; Osborn, D. L. *J. Phys. Chem. A* **2008**, *112*, 9366.
(32) Wang, J.; Yang, B.; Cool, T. A.; Hansen, N.; Kasper, T. To be published.
(33) Whiting, E. E. *J. Quant. Spectrosc. Radiat. Transfer* **1968**, *8*, 1379.
(34) Davis, S. J.; Mulhall, P. A.; Bachman, M.; Kessler, W. J.; Keating, P. B. *J. Phys. Chem. A* **2002**, *106*, 8323.
(35) Burde, D. H.; McFarlane, R. A. *J. Chem. Phys.* **1976**, *64*, 1850.
(36) Deakin, J. J.; Husain, D. *J. Chem. Soc., Faraday Trans. 2* **1972**, *68*, 41.
(37) Deakin, J. J.; Husain, D. *J. Chem. Soc., Faraday Trans. 2* **1972**, *68*, 1603.
(38) Shafir, E. V.; Slagle, I. R.; Knyazev, V. D. *J. Phys. Chem. A* **2003**, *107*, 8893.
(39) Ianni, J. C. *Kintecus*, version 3.9; 2006; http://www.kintecus.com.
(40) Bobeldijk, M.; van der Zande, W. J.; Kistemaker, P. G. *Chem. Phys.* **1994**, *179*, 125.
(41) Yamasaki, K.; Watanabe, A. *Bull. Chem. Soc. Jpn.* **1997**, *70*, 89.
(42) Yamasaki, K.; Watanabe, A.; Kakuda, T.; Tokue, I. *Int. J. Chem. Kinet.* **1998**, *30*, 47.
(43) Tsang, W.; Hampson, R. F. *J. Phys. Chem. Ref. Data* **1986**, *15*, 1087.
(44) Klippenstein, S. J.; Georgievskii, Y.; Harding, L. B. *Phys. Chem. Chem. Phys.* **2006**, *8*, 1133.
(45) Stoliarov, S. I.; Knyazev, V. D.; Slagle, I. R. *J. Phys. Chem. A* **2000**, *104*, 9687.
(46) Slagle, I. R.; Gutman, D.; Davies, J. W.; Pilling, M. J. *J. Phys. Chem.* **1988**, *92*, 2455.
(47) Chambreau, S. D.; Lemieux, J.; Wang, L.; Zhang, J. *J. Phys. Chem. A* **2005**, *109*, 2190.
(48) Robinson, J. C.; Harris, S. A.; Sun, W.; Sveum, N. E.; Neumark, D. M. *J. Am. Chem. Soc.* **2002**, *124*, 10211.
(49) Lee, H.-Y.; Kislov, V. V.; Lin, S.-H.; Mebel, A. M.; Neumark, D. M. *Chem.—Eur. J.* **2003**, *9*, 726.
(50) Doering, J. P.; McDiarmid, R. *J. Chem. Phys.* **1980**, *73*, 3617.
(51) Saha, B.; Ehara, M.; Nakatsuji, H. *J. Chem. Phys.* **2006**, *125*, 014316.
(52) Klippenstein, S. J.; Harding, L. B. *Phys. Chem. Chem. Phys.* **1999**, *1*, 989.
(53) DeSain, J. D.; Taatjes, C. A. *J. Phys. Chem. A* **2003**, *107*, 4843.
(54) Knyazev, V. D.; Slagle, I. R. *J. Phys. Chem. A* **2001**, *105*, 3196.
(55) Atkinson, D. B.; Hudgens, J. W. *J. Phys. Chem. A* **1999**, *103*, 4242.
(56) Hanning-Lee, M. A.; Pilling, M. J. *Int. J. Chem. Kinet.* **1992**, *24*, 271.

JP8096132